

# A Modified Fourier Transform Method for Multiple Scattering Calculations in a Plane Parallel Mie Atmosphere

J. V. Dave and J. Gazdag

A method for evaluating characteristics of the scattered radiation emerging from a plane parallel atmosphere containing large spherical particles is described. In this method, the normalized phase function for scattering is represented as a Fourier series whose maximum required number of terms depends upon the zenith angles of the directions of incident and of scattered radiation. Some results are presented to show that this method can be used to obtain reliable numerical values in a reasonable amount of computer time.

## I. Introduction

Reliable evaluation of the characteristics of the radiation scattered by a planetary atmosphere runs into serious difficulties, especially when the atmospheric model under investigation is nonhomogeneous in the vertical and contains particles that are large compared to the wavelength of interest. Basically, the computational problem reduces to that of performing several iterations and that of evaluating several thousands of integrals at each stage of iteration. When the normal scattering optical thickness of the atmosphere is of the order of unity, one may have to deal with data sets consisting of several million words and may have to perform anywhere from two to twenty iterations depending upon the desired accuracy. Even though one might obtain a reliable numerical solution for a single case at the cost of several hundred hours of computer time, the results so obtained are of very little practical value unless further results are also obtained for several hundred other cases generated by varying input parameters. Thus, it is essential to develop and to use computational procedures which can provide results of highest reliability with a minimum of computer time. Because of this, considerable effort has been directed toward development of acceptable models in which the scattering phase function and/or the vertical nonhomogeneity are so approximated as to permit some analytic reduction.<sup>1-3</sup> However, such attempts have met with only limited success.

A direct numerical solution of the equation of radiative transfer for a plane parallel, nonhomogeneous Mie

atmosphere without any approximation to phase function and/or vertical nonhomogeneity can be obtained by appealing to Monte Carlo methods. However, because of the excessive computer time requirements, published results<sup>4-6</sup> are of marginal reliability at the most and fail to throw much light on the effect of multiple scattering on some salient features of the scattering phase function. In fact, it appears that much more reliable results can be obtained by using a straightforward computational method in which all three integrations (over azimuth angle, over zenith angle, and over optical depth) are carried out numerically with rather crude integration increments, e.g., 30° over azimuth.<sup>7-9</sup>

The computational task is considerably simplified by expressing the phase function in the form of a Fourier series in terms of the difference between azimuth angles of the directions of incidence and of scattering. When this can be done, integration over azimuth can be carried out analytically. This has been used with great advantage for obtaining numerical solutions to multiple scattering problems in plane parallel, molecular atmospheres where the Fourier series can be terminated after the first three terms. When particles large compared to the wavelength of interest are present (Mie scattering if particles are assumed to be spherical), a meaningful representation of the phase function is obtained only after including several tens to several hundreds of terms, depending upon the model. Hence, a Fourier series approach to multiple scattering calculations in the presence of large particles has been generally thought of as unattractive (e.g., Ref 10).

Chandrasekhar<sup>11</sup> showed that a solution of the equation of transfer for a plane parallel, homogeneous atmosphere can be obtained in the  $n$ th approximation by expressing a general phase function in the form of a Fourier series. Twomey *et al.*<sup>12</sup> used the matrix method (or an equivalent of van de Hulst's doubling method<sup>13</sup>) cou-

The authors are with the IBM Scientific Center, Palo Alto, California 94304.

Received 3 December 1969.

pled with a Fourier representation of the phase function technique to simplify the task of multiple scattering calculations for a homogeneous case. However, almost all of their published results<sup>12,14,15</sup> are for the first term of the Fourier series only, i.e., for the intensities of the emergent radiation averaged over azimuth. Because of this usefulness of their published results is very limited. Very recently, Hansen<sup>16,17</sup> has published some results of his extensive computations of radiation emerging from plane parallel, homogeneous Mie atmospheres using Van de Hulst's doubling method. He has expanded the phase function in a Fourier series with as many as 180 terms for some models which contain fairly large particles and has used all these terms in his computations.

The purpose of this paper is to show that multiple scattering calculations can be simplified still further by using a modified form of the Fourier series in which advantage is taken of the fact that the maximum required number of terms in the series is also a function of zenith angles of the directions of incidence and scattering. The results of the scattered radiation emerging from homogeneous Mie atmospheres presented here are obtained by using an iterative procedure in which the  $n$ th approximation amounts to using up to and including  $n$ th orders of scattering.<sup>18,19</sup>

## II. Modified Fourier Series for the Phase Function

### A. General

Let a direction be represented by its zenith angle  $\theta$  [ $=\cos^{-1}|\mu|$ ] and its azimuth angle  $\varphi$  referred to an arbitrary vertical plane. Let  $(\mu, \varphi)$  and  $(\mu', \varphi')$  be, respectively, the directional parameters of the scattered and of the incident radiations. The normalized scattering phase function  $P[\mu, \mu', (\varphi' - \varphi)]$  for a unit volume containing an arbitrary size distribution of spherical particles of known refractive index can be expressed in the form of a Fourier series as follows:

$$P[\mu, \mu', (\varphi' - \varphi)] = \sum_{n=1}^N F_n(\mu', \mu) \cos(n-1)(\varphi' - \varphi). \quad (1)$$

It should be noted that the coefficients  $F_n(\mu', \mu)$  are also functions of the size distribution parameters and the refractive index  $m$  of the material of the sphere with respect to its surroundings.  $N$ , the maximum number of terms after which the series can be terminated, is approximately  $2x_2 + 10$ , where  $x_2$  is the size parameter of the largest particle in the model ( $x = 2\pi r/\lambda$ ,  $r$  is radius, and  $\lambda$  is the wavelength of the radiation under investigation). For Rayleigh scattering,  $N = 3$  and the coefficients are expressible in terms of  $\mu$  and  $\mu'$  as follows:

$$F_1(\mu', \mu) = \frac{3}{8} (3 - \mu^2 - \mu'^2 + 3\mu^2\mu'^2), \quad (2)$$

$$F_2(\mu', \mu) = \frac{3}{2} \mu\mu'(1 - \mu^2)^{\frac{1}{2}}(1 - \mu'^2)^{\frac{1}{2}}, \quad (3)$$

and

$$F_3(\mu', \mu) = \frac{3}{8} (1 - \mu^2)(1 - \mu'^2). \quad (4)$$

The highest number of terms ( $\doteq 2x_2 + 10$ ) in the series should be required for the case  $\mu = \mu' = 0$ , i.e.,

when one has to make use of the entire phase function curve from scattering angle  $\theta = 0^\circ$  to  $\theta = 180^\circ$ . The phase function  $P[\mu, \mu', (\varphi' - \varphi)]$  is fully representable by only one term of the series when  $\mu$  and/or  $\mu' = \pm 1$ , i.e.,  $N$  is equal to unity. For intermediate cases, all  $F_n(\mu', \mu)$  do exist, but  $F_n(\mu', \mu)$  decreases with  $n$ , and hence it should be possible to represent  $P[\mu, \mu', (\varphi' - \varphi)]$  with some desired accuracy by  $N(\mu', \mu)$  number of terms such that  $N(\mu', \mu)$  is less than  $N$ . Thus in the modified Fourier method, we shall represent the normalized phase function for scattering as follows:

$$P[\mu, \mu', (\varphi' - \varphi)] = \sum_{n=1}^{N(\theta', \theta)} F_n(\theta', \theta) \cos(n-1)(\varphi' - \varphi). \quad (5)$$

The parameters of  $N$  and  $F_n$  are changed from  $\mu'$  and  $\mu$  to  $\theta'$  and  $\theta$ , respectively, as subsequent multiple scattering calculations are performed with equal increments in zenith angle.

Computation of  $F_n(\theta', \theta)$  and  $N(\theta', \theta)$  were carried out for two different size distribution models referred to as *haze M* and *cloud* by Deirmendjian.<sup>20</sup> The size distribution functions and lower ( $r_1$ ) and upper ( $r_2$ ) limits of integration used in these computations are as follows:

$$\begin{aligned} \text{haze M: } n(r) &= 5.33 \times 10^4 r \exp[-8.944(r)^{\frac{1}{2}}], \\ r_1 &= 0.001 \mu \text{ and } r_2 = 7.0 \mu, \end{aligned} \quad (6)$$

and

$$\begin{aligned} \text{cloud: } n(r) &= 2.373r^6 \exp(-1.5r), \\ r_1 &= 0.1 \mu \text{ and } r_2 = 14.0 \mu. \end{aligned} \quad (7)$$

### B. Method of Computations

Values of the normalized phase function at  $0.2^\circ$  interval in  $\theta$  were first obtained by following a procedure outlined elsewhere.<sup>21</sup> An integration increment of  $0.1$  in  $x$  was used for this purpose. Values of  $F_n(\theta', \theta)$  and  $N(\theta', \theta)$  were then obtained from these values by following the procedure outlined below:

(1) For a given set of  $\mu', \mu$ , values of  $P[\mu, \mu', (\varphi' - \varphi)]$  for  $2^j + 1$  equally spaced values of  $\varphi' - \varphi$  in the range  $0^\circ - 180^\circ$  are obtained by linear interpolation.

(2) The values obtained from step (1) are then used to compute  $2^j + 1$  coefficients of the Fourier series using subroutine HARM.<sup>22</sup>

(3) A procedure is then set up to determine how many of the  $2^j + 1$  coefficients are necessary to regenerate  $2^j + 1$  values of  $P[\mu, \mu', (\varphi' - \varphi)]$  with the desired accuracy. If this cannot be achieved by using the first  $2^{(j-1)}$  coefficients, a message to that effect is printed out, and the computations are terminated.

(4) After completing the computations for all  $\mu', \mu$  combinations, the data is rearranged so as to permit access to all coefficients for a given frequency  $n$  by issuing one READ command.

For the case haze M and  $\lambda = 0.75 \mu(x_2 \doteq 58.5$  and

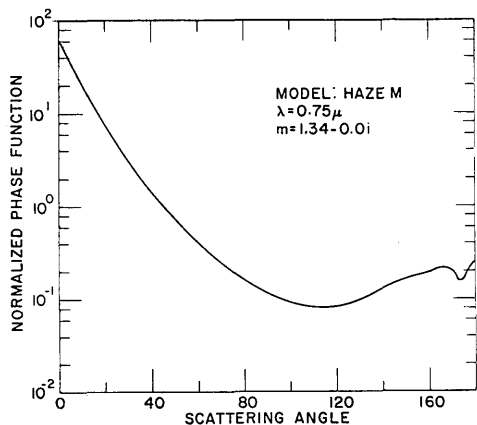


Fig. 1. Normalized phase function for scattering by a polydispersed water spheres model haze M,  $\lambda = 0.75 \mu$ ,  $m = 1.34$ .

$N \doteq 130$ ) for which variations in phase function vs scattering angle are shown in Fig. 1, it was possible to regenerate  $P[\mu, \mu', (\varphi' - \varphi)]$  within  $\pm 0.1\%$  accuracy for all  $\theta', \theta$  combinations given by  $\theta' = 0^\circ(2^\circ)180^\circ$  and  $\theta = 0^\circ(2^\circ)90^\circ$ . The CPU time for all these computations using an IBM System/360 Model 91 computer was about 8.5 min when a value of 8 for  $j$  was used. The accuracy with which such regeneration can be achieved decreases with  $\lambda$  and also when one switches from the haze M to the cloud model. For the case cloud,  $\lambda = 0.45 \mu$  ( $x_2 \doteq 195$ ,  $N \doteq 400$ ),  $P[\mu, \mu', (\varphi' - \varphi)]$  could be regenerated within  $\pm 4.3\%$  only. Such a decrease in stability is partly due to errors inherent in the original scattering function vs scattering angle table.

### C. Results

Values of  $F_n(\theta', \theta)$  for  $\theta = 90^\circ$  and for  $\theta' = 10^\circ, 40^\circ, 60^\circ, 80^\circ$ , and  $90^\circ$  are plotted in Fig. 2 as a function of the subscript  $n$ . For the case haze M,  $\lambda = 0.75 \mu$ , the entire phase function of Fig. 1 can be reproduced within  $\pm 0.1\%$  accuracy with not more than 101 terms. This decrease in the value of  $N$  from 130 to 101 is due to insignificant contributions from extremely large particles in the model under the adopted accuracy criterion. From Fig. 2, it can also be seen that  $N(\theta', 90^\circ)$  decreases from 101 to about 5 as  $\theta'$  is decreased from  $90^\circ$  to  $10^\circ$ .

The variations of  $N(\theta', \theta)$  as a function of  $\theta'$  are presented in Fig. 3 for  $\theta = 20^\circ, 40^\circ, 60^\circ$ , and  $80^\circ$ . For  $\theta = 0^\circ$ ,  $N(\theta', \theta) = 1$  for all values of  $\theta'$ . The striking dependence of  $N(\theta', \theta)$  on the zenith angle of the incident and of the scattered radiation is very evident. All the curves show two maxima; a strong one at  $\theta' = \theta$ , a case for which the scattering angle  $\Theta$  varies from  $0^\circ$  to  $2\theta$ , and a weak one at  $\theta' = 180^\circ - \theta$ , a case for which  $\Theta$  varies from  $180^\circ$  to  $180^\circ - 2\theta$ . Values of  $N(\theta', \theta)$  and

$F_n(\theta', \theta)$  for values of  $\theta$  greater than  $90^\circ$  can be obtained by making use of the following relationships:

$$N(\theta', \theta) = N(180^\circ - \theta', 180^\circ - \theta), \quad (8)$$

and

$$F_n(\theta', \theta) = F_n(180^\circ - \theta', 180^\circ - \theta). \quad (9)$$

### D. Comparison with Results for a Single Particle

The results presented in Figs. 2 and 3 are important enough to warrant a further investigation into the causes which lead to such trends. Consequently, after this study was completed, a considerable amount of work was done to compute values of  $F_n(\theta', \theta)$  and  $N(\theta', \theta)$  directly for a single sphere. The results of this later work are presented elsewhere.<sup>23,24</sup> It was found that as in Fig. 2, the value of  $F_1(90^\circ, 90^\circ)$  for a sphere with size parameter  $x = 100.0$  is less than that of  $F_2(90^\circ, 90^\circ)$ . However, a further increase in  $n$  results in a much less rapid decrease in  $F_n(90^\circ, 90^\circ)$  than the one shown in Fig. 2. This effect results from integration over the size distribution.

Values of  $N(\theta', \theta)$  for a single sphere were obtained directly from computed values of  $F_n(\theta', \theta)$  by using a somewhat different but essentially equivalent criterion. Plots of these values of  $N(\theta', \theta)$  as a function of  $\theta'$  do not show two sharp peaks as is the case of polydispersed aerosol model haze M,  $\lambda = 0.75 \mu$  (Fig. 3). For a single particle, the  $N(\theta', \theta)$  vs  $\theta'$  curve depicts a broad maximum around  $\theta' = 90^\circ$  whose width decreases with increase of  $\theta$ . The values of  $N(90^\circ, \theta)$  increase with  $\theta$ . This difference between the shapes of  $N(\theta', \theta)$  vs  $\theta'$  curves for a single particle and those for polydispersed aerosol model can be partly understood when one takes into account the fact that most of the ripple-like Mie scattering features disappear upon integration over a size distribution. This then implies that the

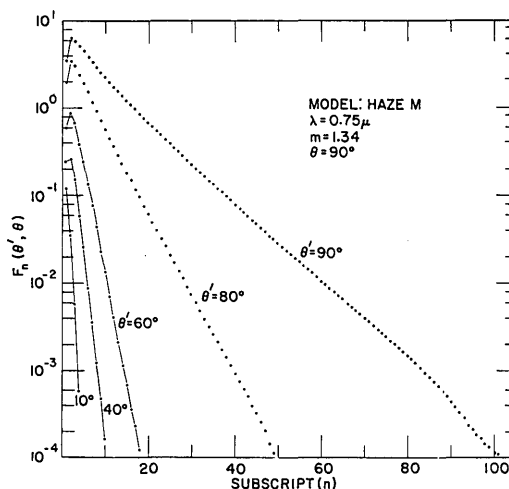


Fig. 2. Variations as a function of subscript  $n$ , of the coefficients  $F_n(\theta', \theta)$  of the fourier series for the normalized phase function in Fig. 1.

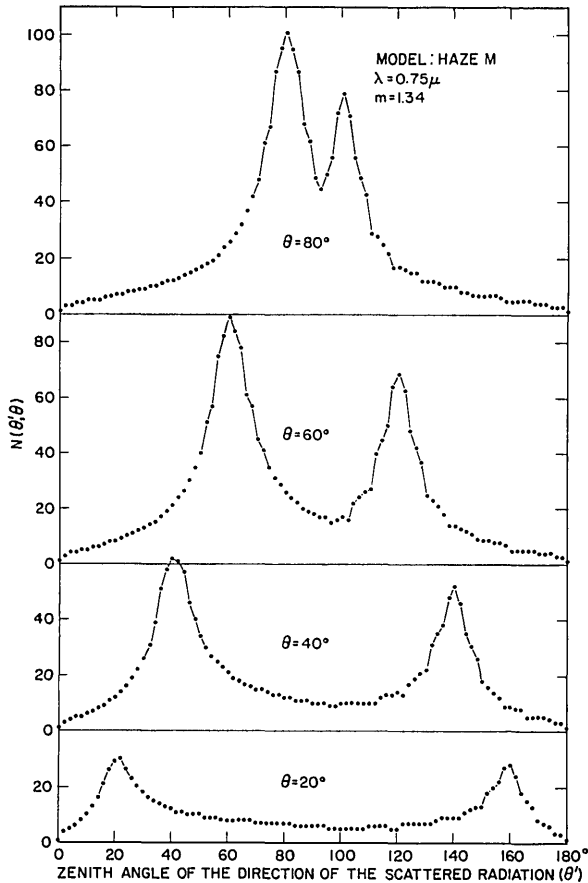


Fig. 3.  $N(\theta', \theta)$ , the number of terms in the fourier series [Eq. (5)] necessary for reproducing a section of phase function curve (Fig. 1) between  $|\theta' - \theta|$  and  $\theta' + \theta$  within  $\pm 0.1\%$  accuracy.

shape of the  $N(\theta', \theta) - \theta'$  curve is also dependent upon size distribution parameters.

### III. Multiple Scattering Calculations

#### A. Necessary Expressions

The equations for the transfer of solar radiation through a plane parallel, nonabsorbing homogeneous atmosphere of finite optical extent in the vertical, but of infinite extent in the horizontal direction, has the following form<sup>11</sup>:

$$\mu \frac{dI(\tau; \mu, \varphi)}{d\tau} = I(\tau; \mu, \varphi) - J(\tau; \mu, \varphi), \quad (10)$$

where  $I(\tau; \mu, \varphi)$  represents the intensity of the scattered radiation emerging at the optical depth  $\tau$  in the direction whose parameters are  $\mu, \varphi$ . A minus (plus) sign before  $\mu$  implies that the scattered radiation is propagating downwards (upwards) in the atmosphere. The source function  $J(\tau; \mu, \varphi)$  is given by

$$J(\tau; \mu, \varphi) = \frac{1}{4} F e^{-\tau/\mu_0} P[\mu, -\mu_0, (\varphi_0 - \varphi)]$$

$$+ \frac{1}{4\pi} \int_{-1}^{+1} \int_0^{2\pi} P[\mu, \mu', (\varphi' - \varphi)] I(\tau; \mu', \varphi') d\mu' d\varphi'. \quad (11)$$

It is assumed that the atmosphere is illuminated at  $\tau = 0$  by unidirectional solar radiation of  $\pi F$  units per unit area normal to the direction of incidence represented by  $-\mu_0, \varphi_0$ . ( $F$  is taken to be unity for the computations presented in this paper.) The boundary conditions are

$$\left. \begin{aligned} I(0; -\mu, \varphi) &\equiv 0 \\ I(\tau_1; +\mu, \varphi) &\equiv 0 \end{aligned} \right\}, \quad (12)$$

which means that there is no scattered radiation illuminating the atmosphere from above its top ( $\tau = 0$ ), or from below its bottom ( $\tau = \tau_1$ ).

When the findings of Sec. II are substituted in Eq. (11), we have the following expression for the first approximation of the source function given by the first term on the right-hand side of Eq. (11):

$$J_1(\tau; \pm\mu, \varphi) = \sum_{n=1}^{N(\theta_0)} J_1^{(n)}(\tau; \pm\mu, -\mu_0) \cos(n-1)(\varphi_0 - \varphi), \quad (13)$$

where

$$J_1^{(n)}(\tau; +\mu, -\mu_0) = \frac{1}{4} F e^{-\tau/\mu_0} F_n(180^\circ - \theta, \theta_0) \quad (14)$$

and

$$J_1^{(n)}(\tau; -\mu, -\mu_0) = \frac{1}{4} F e^{-\tau/\mu_0} F_n(\theta, \theta_0). \quad (15)$$

$N(\theta_0)$  is the maximum value of  $N(\theta, \theta_0)$  vs.  $\theta$  curve for the given solar zenith angle  $\theta_0$ . From Fig. 3, we have  $N(\theta_0) = N(\theta_0, \theta_0)$ . It is true that the number of terms in the series of  $J_1$  [Eq. (13)] is a function of both  $\theta$  and  $\theta_0$ . However, even though it is possible to generate high-frequency components upon multiple scattering, in no case can the number of terms exceed the highest value  $N(\theta_0)$  which is determined by the position of the sun and the atmospheric model under investigation. The intensities of the radiation emerging after one scattering are then given by

$$I_1^{(n)}(\tau; \pm\mu, -\mu_0) = I_1^{(n)}(\tau \pm \Delta\tau; \pm\mu, -\mu_0) e^{-\Delta\tau/\mu} + \bar{J}_1^{(n)}(\tau; \pm\mu, -\mu_0) (1 - e^{-\Delta\tau/\mu}). \quad (16)$$

Equation (16) is arrived at after dividing the homogeneous, nonabsorbing atmosphere into several layers, each of scattering optical thickness  $\Delta\tau$ .  $\bar{J}_1^{(n)}$  is the mean value of the source function in the layer bounded by  $\tau$  and  $\tau - \Delta\tau$  or  $\tau + \Delta\tau$  as the case may be. From Eq. (12) we have,

$$I_1^{(n)}(0; -\mu, -\mu_0) \equiv I_1^{(n)}(\tau_1; +\mu, -\mu_0) \equiv 0. \quad (17)$$

Evidently,

$$I_1(\tau; \pm\mu, \varphi) = \sum_{n=1}^{N(\theta_0)} I_1^{(n)}(\tau; \pm\mu, -\mu_0) \times \cos(n-1)(\varphi_0 - \varphi). \quad (18)$$

The values of  $I_1$  given by Eq. (18) and those of  $P[\mu, \mu', (\varphi' - \varphi)]$  given by Eq. (5) are then substituted in the double integral on the right-hand side of Eq. (11).

After integrating over  $\varphi'$  from 0 to  $2\pi$ , we have the following result:

$$\begin{aligned} & \frac{1}{4\pi} \int_{-1}^{+1} \int_0^{2\pi} P[\mu, \mu', (\varphi' - \varphi)] I_{m-1}(\tau; \mu', \varphi') d\mu' d\varphi' \\ &= \frac{1}{4} \left[ \sum_{n=1}^{N(\theta_0)} (1 + \delta_{1n}) \int_0^1 F_n(-\mu', \mu) I_{m-1}^{(n)}(\tau; -\mu', -\mu_0) d\mu' \right. \\ & \quad \left. + \sum_{n=1}^{N(\theta_0)} (1 + \delta_{1n}) \int_0^1 F_n(\mu', \mu) I_{m-1}^{(n)}(\tau; \mu', -\mu_0) d\mu' \right] \\ & \quad \times \cos(n-1)(\varphi_0 - \varphi). \quad (19) \end{aligned}$$

As discussed above, Eq. (19) is valid for  $m = 2$  only. However, by repeated substitution, it can be shown that Eq. (19) as well as all subsequent equations are valid for  $m \geq 2$ . The quantity  $\delta_{1n}$  is the Kronecker delta function given by  $\delta_{1n} = 1$  when  $n = 1$  and otherwise zero.

For integration over  $\mu'$ , the interval of integration is divided into equal increments in  $\theta'$ . This is advisable for large particle scattering where the properties vary rapidly with scattering angle. This change in variable can be accommodated by use of the trapezoidal rule of integration with unequal intervals in  $\mu'$ . We therefore have

$$J_m(\tau; \pm\mu, \varphi) = \sum_{n=1}^{N(\theta_0)} J_m^{(n)}(\tau; \pm\mu, -\mu_0) \times \cos(n-1)(\varphi_0 - \varphi), \quad (20)$$

where

$$\begin{aligned} J_m^{(n)}(\tau; -\mu, -\mu_0) &= J_1^{(n)}(\tau; -\mu, -\mu_0) \\ &+ \frac{1}{4} (1 + \delta_{1n}) \sum_{i=i_2(n,\theta)}^{i_1(n,\theta)} \langle F_n(180^\circ - \theta'_i, \theta) I_{m-1}^{(n)}(\tau; +\mu'_i, -\mu_0) \rangle \\ &\times (\mu'_i - \mu'_{i+1}) + \frac{1}{4} (1 + \delta_{1n}) \sum_{i=i_1(n,\theta)}^{i_2(n,\theta)} \langle F_n(\theta'_i, \theta) I_{m-1}^{(n)}(\tau; -\mu'_i, \\ & \quad -\mu_0) \rangle (\mu'_i - \mu'_{i+1}) \quad (21) \end{aligned}$$

and

$$\begin{aligned} J_m^{(n)}(\tau; +\mu, -\mu_0) &= J_1^{(n)}(\tau; +\mu, -\mu_0) \\ &+ \frac{1}{4} (1 + \delta_{1n}) \sum_{i=i_1(n,\theta)}^{i_2(n,\theta)} \langle F_n(\theta'_i, \theta) I_{m-1}^{(n)}(\tau; +\mu'_i, -\mu_0) \rangle (\mu'_i - \mu'_{i+1}) \\ &+ \frac{1}{4} (1 + \delta_{1n}) \sum_{i=i_2(n,\theta)}^{i_1(n,\theta)} \langle F_n(180^\circ - \theta'_i, \theta) I_{m-1}^{(n)}(\tau; -\mu'_i, \\ & \quad -\mu_0) \rangle (\mu'_i - \mu'_{i+1}). \quad (22) \end{aligned}$$

The angle brackets around the quantities under the summation sign represent the mean value of the quantity for the interval  $\mu'_i - \mu'_{i+1}$ . The subscript  $i$  is assumed to increase continuously from unity at zenith (or nadir) to its maximum value at the horizon. The values of the limits, i.e.,  $i_1(n, \theta)$ , etc., can be found by consulting variations of  $N(\theta', \theta)$  vs  $\theta'$ .

Having obtained values of  $J_2^{(n)}(\tau; \pm\mu, -\mu_0)$ , the values of  $I_2^{(n)}(\tau; \pm\mu, -\mu_0)$  and  $I_2(\tau; \pm\mu, \varphi)$  can be obtained by making use of the equations obtained after replacing subscript 1 by 2 in Eqs. (16)–(18).  $I_2(\tau; \pm\mu, \varphi)$  so obtained contains radiation which emerges after suffering up to and including two scatterings.

Equations (20)–(22) and the appropriately modified

forms of Eqs. (16)–(18) can then be used to include further higher orders of scattering ( $m > 2$ ).

## B. Computational Details

The equations given in Sec. III.A were used to compute the intensity of the radiation emerging at various levels of a plane parallel, nonabsorbing, Mie atmosphere. For this purpose, the atmospheric model was divided into several layers, each having a thickness ( $\Delta\tau$ ) of 0.01. For integration over  $\mu'$ , the angular region from zenith to nadir was divided into  $2^\circ$  intervals ( $\Delta\theta$ ). Values of the quantity  $\bar{J}_m^{(n)}(\tau; \pm\mu, -\mu_0)$  were obtained by taking the mean values of the appropriate source function [Eqs. (20)–(22)] at the top and at the bottom of the atmosphere. The values of  $I_m^{(n)}(\tau; 0, 0, -\mu_0)$  were obtained by linear extrapolation. The iterative procedure outlined above and used in these computations is referred to as a *successive scattering* iterative procedure, since each higher approximation amounts to including one more order of scattering. The iteration procedure was terminated when successively iterated values of  $I_m^{(n)}(\tau_1; -\mu, -\mu_0)$  and  $I_{m-1}^{(n)}(\tau_1; -\mu, -\mu_0)$  converged within 0.1% for all values of  $\mu$ .

The upper section of Fig. 4 shows as a function of frequency ( $n$ ) the number of iterations ( $m$ ) required for achieving the desired convergence of the downward radiation at the bottom of the atmosphere when  $\tau_1 = 1.00$  and  $\theta_0 = 60^\circ$ . The quantity  $m$  decreases rapidly

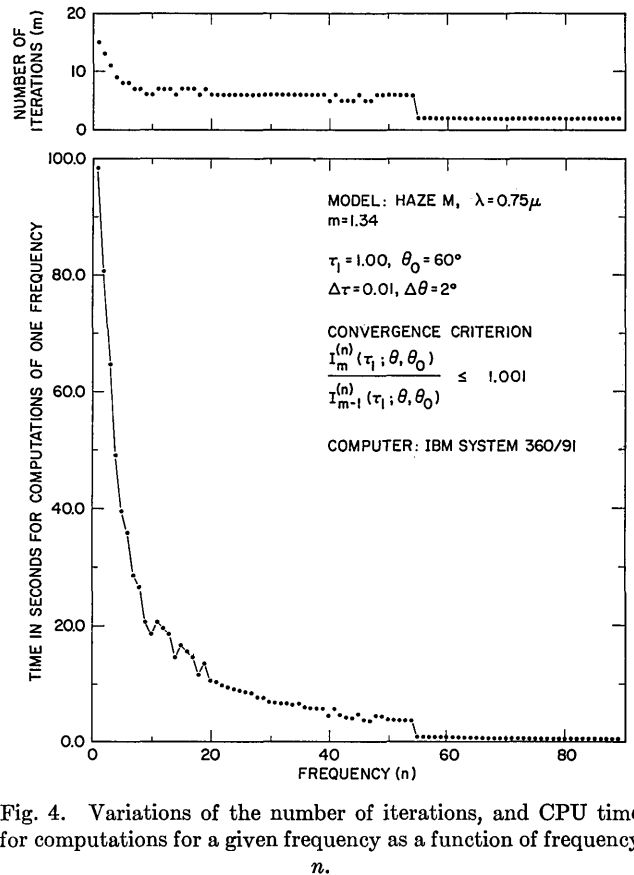


Fig. 4. Variations of the number of iterations, and CPU time for computations for a given frequency as a function of frequency  $n$ .

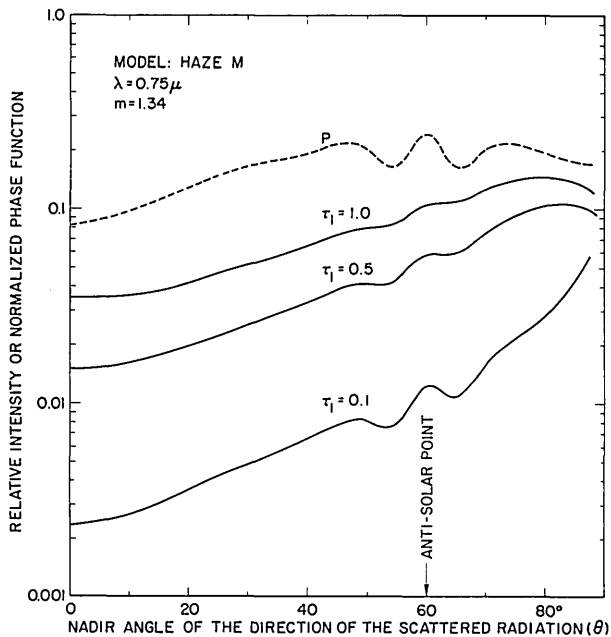


Fig. 5. Variations of the intensity of the radiation backscattered by a plane parallel, homogeneous atmosphere containing spherical polydispersions. Model haze M,  $\lambda = 0.75 \mu$ ,  $m = 1.342 - 0.0i$ . The  $x$  axis represents the nadir angle of the emergent radiation in a vertical plane making an angle of  $180^\circ$  with the sun's vertical plane.  $\theta_0 = 60^\circ$ . The broken curve (marked P) represents the scattering property of a unit volume. Different curves are for the atmospheric models with different values for their normal scattering optical thicknesses. Solar flux incident on the top of the atmosphere =  $\pi$  units per unit area normal to the direction of incidence.

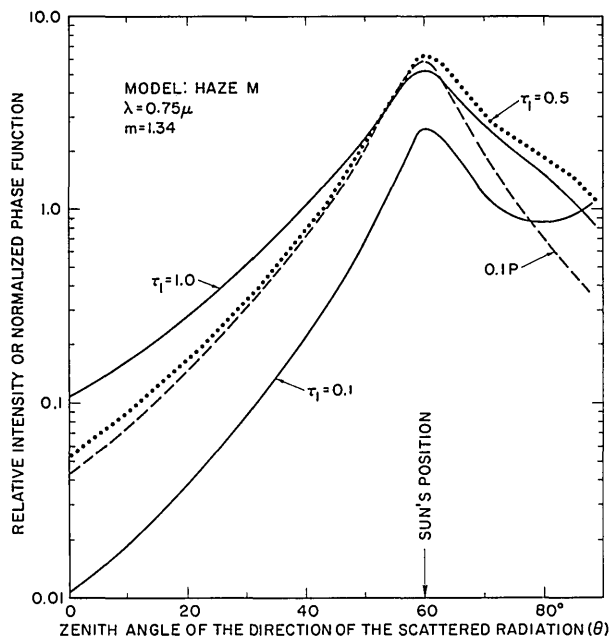


Fig. 6. Same as Figure 5 but for the downward radiation emerging at the bottom of the atmosphere. The  $x$  axis represents the zenith angle of the emergent radiation in the sun's vertical plane.

from 15 at  $n = 1$  to a value of about 6 at  $n = 10$ . It shows very little change for further increase of  $n$  from 10 to 55. For still higher values of  $n$ ,  $m = 2$ . Such dependence of  $m$  on  $n$  can be anticipated from similar results for Rayleigh scattering calculations published by Dave and Walker.<sup>19</sup>

The CPU time for computations at one frequency decreases much more rapidly with increase of  $n$  (lower section of Fig. 4). When computations are performed with  $\Delta\theta = 2^\circ$  and  $\Delta\tau = 0.01$ , about 98 sec of CPU time are required for computations at  $n = 1$  on an IBM System/360 Model 91 computer. For  $n = 10$ , it is about 20 sec. Because of a rapid decrease in numerical work involved in the computations of the source function, CPU time decreases rapidly from 20 sec to 4 sec in the frequency domain where  $m$  is constant. For still higher values of  $n$ , it takes about 0.4 sec of CPU time for all computations for a given  $n$ .

The total CPU time required for the entire calculation is about 3 min for  $\theta_0 = 0^\circ$ , for which it is necessary to compute at one frequency only, and about 13 min for  $\theta_0 = 60^\circ$ , for which computations have to be carried out for eighty-nine frequencies. This total CPU time includes the following: (1) computations of upward and downward fluxes at 101 levels; (2) intensities of the upward and downward radiation at  $\tau = 0, \tau_1/2$  and  $\tau_1$  for  $\theta = 0^\circ(2^\circ)90^\circ$  and  $\varphi_0 - \varphi = 0^\circ(1^\circ)180^\circ$ , and (3) execution of a very substantial number of printout statements.

It was noted that the time quoted above decreases by factors of about eight and twenty when computations are carried with  $6^\circ$  and  $10^\circ$  increment in the zenith angle, respectively. This time can be reduced still further by relaxing the present convergence criterion.

### C. Tests for Reliability

The reliability of the numerical results obtained with the present method can be checked to some extent by comparing the values obtained for a Rayleigh case with those obtained with Chandrasekhar's method<sup>11</sup> ( $X$  and  $Y$  functions) where integrations over both optical depth and azimuth are performed analytically. However, the published numerical results using Chandrasekhar's method are for a Rayleigh atmosphere in which the polarization of the scattered radiation is also taken into account, i.e., a phase matrix treatment. Apart from the significant differences between the values obtained with the phase matrix and phase function treatments, reliable comparison is hampered due to the fact that tabulated values are generally not available for the desired parameters. Because of these reasons, radiation emerging from an atmosphere scattering according to a Rayleigh phase function was calculated by modifying a similar Rayleigh phase matrix computer program discussed elsewhere.<sup>25</sup>

Some results of a comparison are presented in Table I for the radiation emerging from the bottom of a Rayleigh atmosphere with  $\tau_1 = 1.0$  and illuminated by the sun at  $86^\circ$  from the zenith. For a meaningful comparison, it is desirable to select a case like this where the contribution due to higher orders ( $m > 1$ ) of scattering

**Table I. Intensity of the Radiation Emerging at the Bottom of a Plane Parallel, Nonabsorbing, Rayleigh Atmosphere as Obtained Using Three Different Computational Procedures<sup>a</sup>**

$\theta$	$\mu$	Method		
		Chandrasekhar's method		Modified fourier transform method
		Phase matrix	Phase function	
0.0°	1.00	0.01571	0.01755	0.01748
20.0	0.94	0.01785	0.01893	0.01886
36.0	0.81	0.02150	0.02127	0.02120
44.0	0.72	0.02360	0.02254	0.02246
48.0	0.67	0.02457	0.02308	0.02300
60.0	0.50	0.02632	0.02360	0.02350
64.0	0.44	0.02612	0.02307	0.02295
70.0	0.34	0.02436	0.02098	0.02094
72.0	0.31	0.02344	0.02002	0.01989
78.0	0.21	0.01922	0.01594	0.01576
82.0	0.14	0.01601	0.01305	0.01295
86.0°	0.07	0.01358	0.01103	0.01096

Note: Computations using Chandrasekhar's method were carried out for the zenith variables  $\mu$  and  $\mu_0$ , while those using the modified Fourier method were performed for the zenith variables  $\theta$  and  $\theta_0$ .

<sup>a</sup>  $\tau_1 = 1.0, \theta_0 = 86.0^\circ, \mu_0 = 0.07, \varphi_0 - \varphi = 0^\circ$ .

is at least two to three times that due to primary scattering alone.<sup>26</sup> From Table I it can be seen that numerical solutions of the radiative transfer equation as obtained using the Rayleigh phase matrix (column 3) and the Rayleigh phase function (column 4) can differ by as much as 23% in some cases. Hence, for a meaningful comparison, it is essential to use exactly the same scattering law for all test cases. Because of the differences in quadrature procedures, values given in Table I for Chandrasekhar's method are for the zenith distances given by  $\mu$  and  $\mu_0$ , while those for the method described in this paper are for zenith distances given by  $\theta$  and  $\theta_0$ . The values of  $\theta$  as obtained from  $\cos^{-1}\mu$  differ by about  $\pm 0.1^\circ$  from the corresponding values given in column 1. A comparison of the values given in the last two columns shows that the values for a Rayleigh case as obtained from use of the modified fourier transform method are good to three significant figures when values of 0.01 and  $2^\circ$  for integration increments over  $\tau$  and  $\theta$ , respectively, are used.

The above finding may not hold true for computations in Mie atmospheres where the phase function changes much more rapidly with the scattering angle. Some confidence in this direction can be gained by examining the net flux  $\Phi(\tau)$  given by

$$\Phi(\tau) = \pi\mu_0 e^{-\tau/\mu_0} + 2\pi \int_0^1 I^{(0)}(\tau; -\mu, -\mu_0)\mu d\mu - 2\pi \int_0^1 I^{(0)}(\tau; +\mu, -\mu_0)\mu d\mu. \quad (23)$$

For a nonabsorbing atmosphere  $\Phi(\tau)$  should be inde-

pendent of  $\tau$ . For a zenith sun, the mean value of  $\Phi(\tau)$  decreases from about 3.0 to 2.1 for the Rayleigh atmosphere, and from about 3.1 to 2.9 for the Mie atmosphere as  $\tau_1$  is increased from 0.1 to 1.0. A decrease in the value of  $\Phi(\tau)$  with  $\tau_1$  is due to an increase in the reflecting power of the atmosphere with  $\tau_1$ . Because of the strong forward peak in the phase function vs scattering angle diagram (Fig. 1), the reflecting power of a Mie atmosphere is somewhat smaller than an equivalent Rayleigh atmosphere. For  $\theta_0 = 60^\circ$ , the mean value of  $\Phi(\tau)$  decreases from about 1.4 to 0.8 for the Rayleigh atmosphere, and from about 1.5 to 1.2 for the Mie atmosphere as  $\tau_1$  is increased from 0.1 to 1.0.

In Table II, we have presented the difference between the maximum and minimum values of  $\Phi(\tau)$  for  $\tau_1 = 0.1$  and 1.0, and  $\theta_0 = 0^\circ$  and  $60^\circ$  when computations are performed with different integration increments in  $\tau$  and  $\theta$ . This difference can be thought of as an upper limit of absolute error. When the increment  $\Delta\tau$  is halved from 0.01 to 0.005, this difference remains unaffected. Furthermore, when a value of  $2^\circ$  for  $\Delta\theta$  is used, the highest error of about one part in 300 is encountered for case B,  $\tau_1 = 1.0$  and  $\theta_0 = 0^\circ$ . Thus, it appears that an increase in value of  $\Delta\tau$  from 0.01 to 0.02 should also give fairly reliable numerical results<sup>8</sup> if the atmosphere is homogeneous and  $\tau_1$  is of the order of unity or less.

An increase in the value of  $\Delta\theta$  from  $2^\circ$  to  $10^\circ$  results in about a thirty-fold increase in the values of this difference. The worst case is encountered when a Mie atmosphere with  $\tau_1 = 1.0$  is illuminated by the sun at zenith. This is because of the appearance of a halo around the sun. In the Mie case, errors decrease with increase in  $\theta_0$  as values of diffuse fluxes are obtained after taking normal components of the intensities according to Eq. (23).

From the results presented above, we see that use of  $\Delta\tau \doteq 0.01$  and  $\Delta\theta \doteq 2^\circ$  provides numerical results that are reliable to within three significant figures. This finding is valid when the scattering optical thickness is of the order of unity or less, and the phase function is not much more strongly peaked than the one shown in Fig. 1. For the cloud model [Eq. (7)], it will be necessary to use a value of  $\Delta\theta$  of about  $1^\circ$  or less.

#### D. Discussion of Results

The expressions given in Sec. III.A were used to compute the intensity of the scattered radiation emerging at the top, at the bottom and at the half-way level of a homogeneous Mie atmosphere whose scattering properties are described in Fig. 1. Computations were carried out for three different values of  $\tau_1$  (namely, 0.1, 0.5, and 1.0) and for five different values of  $\theta_0$  given by  $0^\circ(20^\circ)80^\circ$ . The phase function used here is very similar to one of the phase functions used by Hansen<sup>17</sup> who has recently published some results of his extensive calculations of the radiation emerging from homogeneous, haze and cloud type atmospheres. He has given results for several values of  $\tau_1$  between 1 and 32. Reference should also be made of other published results of Hansen,<sup>16</sup> and of Hansen and Cheyney.<sup>27,28</sup>

**Table II. Difference Between the Maximum and Minimum Values of  $\Phi(\tau)$  as Observed Using Different Integration Increments in  $\tau$  and  $\theta'$ <sup>a</sup>**

$\Delta\tau$	$\Delta\theta$ in degrees	$\tau_1$	$\theta_0$ in degrees	Difference between maximum and minimum values of $\Phi(\tau)$ for	
				Case A Rayleigh	Case B haze $M$ , $\lambda = 0.75 \mu$
0.01	2	0.1	0	0.007	0.0017
0.005	2	0.1	0	0.0006	0.0017
0.005	6	0.1	0	0.007	0.014
0.005	10	0.1	0	0.014	0.038
0.01	2	1.0	0	0.001	0.013
0.005	2	1.0	0	0.001	0.013
0.005	6	1.0	0	0.01	0.11
0.005	10	1.0	0	0.02	0.32
0.005	2	0.1	60	0.0008	0.0006
0.005	6	0.1	60	0.009	0.007
0.005	10	0.1	60	0.02	0.012
0.005	2	1.0	60	0.0014	0.0013
0.005	6	1.0	60	0.010	0.006
0.005	10	1.0	60	0.016	0.014

<sup>a</sup> Maximum number iterations performed: 6 for  $\tau_1 = 0.1$ , 15 for  $\tau_1 = 1.0$ .

Because of this, and as the primary purpose of this paper is to put forward a new computational procedure, the discussion of the results will be kept to a bare minimum.

The variations of the intensity of the radiation emerging at the top of the atmosphere are shown in Fig. 5 for  $\tau_1 = 0.1, 0.5$ , and  $1.0$  and  $\theta_0 = 60^\circ$ . For the vertical plane containing the antisolar point ( $\varphi_0 - \varphi = 180^\circ$ ), scattering by a unit volume (broken curve marked *P*) shows a maximum at  $60^\circ$  preceded as well as followed by a minimum and another equally strong maximum. This is due to the presence of the so-called

glory feature in the original scattering diagram (Fig. 1). This glory feature stands out very clearly in the intensity distribution of the radiation backscattered by an atmosphere of optical thickness  $0.1$  in spite of a strong increase in brightness from nadir to horizon. Remnants of the glory can be clearly seen for  $\tau_1 = 0.5$  and  $1.0$  in the forms of sharp changes in the slopes of intensity vs nadir angle curves. When the computations are performed with  $\Delta\theta = 10^\circ$ , the individual values so obtained (Tables III and IV) agree within 10% with more exact values obtained with a  $2^\circ$  interval. However, because of the sparseness of the data points, it would be very difficult to identify any glory feature with reasonable confidence when the entire computations are carried out with a  $10^\circ$  angular increment.

Similar results for the intensity of the radiation emerging at the bottom of the atmosphere, but for the sun's vertical plane ( $\varphi_0 - \varphi = 0^\circ$ ) are presented in Fig. 6. The important features are the changes in the slope in the forward peak region, and a strong increase in limb darkening as  $\tau_1$  increases from  $0.1$  to  $1.0$ . Both these features are evidently due to the nature of the phase function. They are completely absent in the characteristics of the radiation scattered by a Rayleigh atmosphere under otherwise similar circumstances.

### E. Possible Improvements

The results presented in Sec. III.C can be used as a guide during the development of a computer program aimed at obtaining results of desired accuracy with a minimum of computer time. One can further reduce the computational task by relaxing the convergence criterion used in this paper and also by using gaussian quadrature.<sup>16,17</sup> Further computations with  $\tau_1 = 1.0$  and  $2.0$  showed that the present convergence criterion is not an ideal one. When the propagation of truncation errors cannot permit the achievement of the desired convergence, further iterations lead to less reliable results. This can be avoided by terminating the itera-

**Table III. Intensity of the Radiation Emerging at the Top of a Plane Parallel Atmosphere as Obtained Using  $2^\circ$  and  $10^\circ$  Angular Increments for Integration over Zenith Angle. Solar Flux  $\pi$  Units per Unit Area Normal to the Direction of the Incident Radiation<sup>a</sup>**

Nadir angle $\theta$	$\tau_1 = 0.1$		$\tau_1 = 1.0$	
	$\Delta\theta = 2^\circ$	$\Delta\theta = 10^\circ$	$\Delta\theta = 2^\circ$	$\Delta\theta = 10^\circ$
0	0.00234	0.00225	0.0348	0.0358
10	0.00267	0.00259	0.0358	0.0360
20	0.00357	0.00349	0.0414	0.0414
30	0.00487	0.00478	0.0510	0.0509
40	0.00647	0.00634	0.0639	0.0638
50	0.00817	0.00797	0.0795	0.0797
60	0.0123	0.0120	0.105	0.105
70	0.0157	0.0149	0.126	0.127
80	0.0279	0.0257	0.145	0.145

<sup>a</sup> Model: haze  $M$ ,  $\lambda = 0.75 \mu$ ,  $m = 1.34 - 0.0i$ ,  $\theta_0 = 60^\circ$ ,  $\varphi_0 - \varphi = 180^\circ$ .

**Table IV. Intensity of the Radiation Emerging at the Bottom of a Plane Parallel Atmosphere as Obtained Using  $2^\circ$  and  $10^\circ$  Angular Increments for Integration over Zenith Angle. Solar Flux  $\pi$  Units per Unit Area Normal to the Direction of the Incident Radiation<sup>a</sup>**

Zenith angle $\theta$	$\tau_1 = 0.1$		$\tau_1 = 1.0$	
	$\Delta\theta = 2^\circ$	$\Delta\theta = 10^\circ$	$\Delta\theta = 2^\circ$	$\Delta\theta = 10^\circ$
0	0.0107	0.0107	0.104	0.110
10	0.0192	0.0191	0.164	0.166
20	0.0383	0.0381	0.278	0.279
30	0.0849	0.0846	0.509	0.510
40	0.214	0.214	1.01	1.01
50	0.690	0.690	2.29	2.29
60	2.47	2.47	5.38	5.44
70	1.24	1.24	2.74	2.73
80	0.850	0.823	1.51	1.47

<sup>a</sup> Model: haze  $M$ ,  $\lambda = 0.75 \mu$ ,  $m = 1.34 - 0.0i$ ,  $\theta_0 = 60^\circ$ ,  $\varphi_0 - \varphi = 0^\circ$ .

**Table V. Number of Iterations Needed for Obtaining a Four Significant Figure Convergence of the Diffuse Downward Flux at the Bottom of a Nonabsorbing, Mie Atmosphere<sup>a</sup>**

$\tau_1$	$\theta_0$ in degrees	Maximum number of iterations	
		Gauss-Seidel method	Successive scattering method
0.1	0	5	7
0.5	0	6	9
1.0	0	9	13
2.0	0	14	22
1.0	84	13	19
2.0	84	17	26

<sup>a</sup> Model: haze  $M$ ,  $\lambda = 0.75 \mu$ ,  $\Delta\theta = 2^\circ$ ,  $\Delta\tau = 0.01$ .

tion when the successively iterated values of diffuse downward flux at the bottom of the atmosphere show convergence in the fourth significant place. An upper limit for the number of iterations can be thus obtained during computations for  $n = 1$ , which can be then used during computations for higher frequencies.

One can reduce the computation time still further by making use of a more efficient iteration procedure such as Gauss-Seidel iteration,<sup>29</sup> used extensively by Herman and Browning.<sup>8</sup> This was done and it was found that equally reliable results can be obtained with a significant reduction in computer time (Table V). It should be noted that most of the time is spent in the evaluation of the source function given by Eqs. (20)–(22). Hence, in order to obtain best timings, it is necessary to define  $\bar{J}_m^{(n)}$  as the value of the source function at the center of the layer. It should be further noted that the computations of the first approximation in the successive scattering method take very little time, while those in the Gauss-Seidel method take a very significant amount.

Still another method of saving computer time is to combine the modified fourier method with Van de Hulst's doubling method.<sup>13</sup> A considerable amount of computer time can be saved, especially when one is interested in homogeneous atmospheres only. Hansen and Pollack<sup>30</sup> have also put forward such an idea in the appendix of one of their most recent papers.

Since one is forced to use a fairly large number of points during integration over  $\theta'$ , it would be worthwhile to look into the spherical harmonic method<sup>31</sup> for solution of the transfer equation for a given frequency  $n$ . This is a noniterative method and as such its successful use may lead to saving of a substantial amount of computer time. It should be emphasized that all such time-saving alternatives are needed only during computations of  $I^{(n)}(\tau; \pm\mu, -\mu_0)$  corresponding to the first 10–20 terms of the Fourier series (see Fig. 4).

#### IV. Conclusion

In the preceding sections an efficient computing method that can provide reliable values of the intensity of the scattered radiation emerging from a plane parallel,

Mie atmosphere is described in great detail. Some results of computations are also presented to demonstrate the efficiency of this method and reliability of results obtained therefrom. This method is very flexible as the magnitude of computational load is automatically adjusted by analyzing the scattering characteristics of a unit volume, and the position of the sun. The only two parameters which an investigator has to vary for results with a minimum of time are the integration increments used for numerical quadrature over optical depth and zenith angle. It should be now possible to perform reliable multiple scattering calculations for various models containing large particles without using an excessive amount of time and money. It is proposed to extend the method described here for calculations aimed at determining the polarization characteristics of the radiation scattered by a plane parallel, Mie atmosphere.

We would like to take this opportunity to express our sincere thanks to our colleague, B. H. Armstrong, for a careful reading of the original manuscript and for his very helpful comments.

#### References

1. L. M. Romanova, *Opt. Spectrosc.* **13**, 238 (1962).
2. W. M. Irvine, *Astrophys. J.* **142**, 1563 (1965).
3. J. W. Chamberlain and M. B. McElroy, *Astrophys. J.* **144**, 1148 (1966).
4. D. G. Collins, K. Cunningham, and M. B. Wells, "Monte Carlo Studies of Light Transport," Tech. Rep. ECOM-00240-2, Radiation Research Associates, Inc., Fort Worth, Texas (1967).
5. G. N. Plass and G. W. Kattawar, *Appl. Opt.* **7**, 1129 (1968).
6. G. W. Kattawar and G. N. Plass, *Appl. Opt.* **7**, 1519 (1968).
7. B. M. Herman, *J. Geophys. Res.* **70**, 1215 (1965).
8. B. M. Herman and S. R. Browning, *J. Atmos. Sci.* **22**, 559 (1965).
9. B. M. Herman, *Proceedings of the IBM Scientific Computing Symposium on Environmental Sciences* (IBM Data Processing Division, White Plains, New York, 1967), pp. 211–237.
10. W. M. Irvine, *J. Quant. Spectry. Radiative Transfer* **8**, 471 (1968).
11. S. Chandrasekhar, *Radiative Transfer* (Clarendon Press, Oxford, 1950).
12. S. Twomey, H. Jacobowitz, and H. B. Howell, *J. Atmos. Sci.* **23**, 289 (1966).
13. H. C. Van de Hulst, "A New Look at Multiple Scattering," Institute for Space Studies, NASA, New York (1963).
14. S. Twomey, H. Jacobowitz, and H. B. Howell, *J. Atmos. Sci.* **24**, 70 (1967).
15. H. B. Howell, *J. Atmos. Sci.* **25**, 1090 (1968).
16. J. E. Hansen, *Astrophys. J.* **155**, 565 (1969).
17. J. E. Hansen, *J. Atmos. Sci.* **26**, 478 (1969).
18. J. V. Dave, *Astrophys. J.* **140**, 1292 (1964).
19. J. V. Dave and W. H. Walker, *Astrophys. J.* **144**, 798 (1966).
20. D. Deirmendjian, *Appl. Opt.* **3**, 187 (1964).
21. J. V. Dave, *Appl. Opt.* **8**, 1161, 2153 (1969).
22. "System/360 Scientific Subroutine Package (360A-CM-03X) Version II," Doc. No. H20-0205-02, IBM Technical Publications Dept., White Plains, New York (1966).
23. J. V. Dave and B. H. Armstrong, *J. Quant. Spectry. Radiative Transfer* **10**, No. 6 (1970).
24. J. V. Dave, *Appl. Opt.* **9**, No. 8 (1970).

25. J. V. Dave and R. M. Warten, "Program for Computing the Stokes Parameters of the Radiation Emerging from a Plane-Parallel Non-absorbing, Rayleigh Atmosphere," (Rep. 320-3248, IBM Scientific Center, Palo Alto, Calif., 1968).
26. J. V. Dave, *J. Opt. Soc. Amer.* **54**, 307 (1964).
27. J. E. Hansen and H. Cheyney, *J. Atmos. Sci.* **25**, 629 (1968).

28. J. E. Hansen and H. Cheyney, *J. Geophys. Res.* **74**, 3337 (1969).
29. F. B. Hildebrand, *Introduction to Numerical Analysis* (McGraw-Hill Book Company, Inc., New York, 1956), Chap. 10.
30. J. E. Hansen and J. B. Pollack, *J. Atmos. Sci.* **27**, 265 (1970).
31. V. Kourganoff, *Basic Methods in Transfer Problems* (Clarendon Press, Oxford, 1952).

**Meetings Calendar** continued from page 1452

		<b>May</b>	
4-9	XVI Colloq. Spectroscopicum Internat., Heidelberg <i>W. Fritsche, Ges. Deut. Chem., 6 Frankfurt/Main 8, Postfach 119075, Germany</i>	7-11	Internat. Quantum Electronics Conf., Queen Elizabeth Hotel, Montreal <i>IEEE, 345 E. 47th St., New York, N.Y. 10017</i>
5-8	Optical Society of America, Chateau Laurier, Ottawa <i>J. W. Quinn, OSA, 2100 Pa. Ave., N.W., Wash., D.C. 20037</i>	?	Soc. for Exp. Stress Analysis, Olympic Hotel, Seattle, Wash. <i>SESA, 21 Bridge Sq., Westport, Conn. 06880</i>
18-22	SAS, St. Louis, Mo. <i>J. Westermeyer, Titanium Pigment Div., Nat. Lead Co., Carondelet Sta., St. Louis, Mo. 63111</i>	<b>September</b>	
<b>November</b>		24-29	SMPTE 112th Semiann. Conf., Los Angeles <i>D. A. Courtney, 9 E. 41st St., New York, N.Y. 10017</i>
?	APS, NYC <i>W. W. Havens, Jr., 335 E. 45th St., New York, N.Y. 10017</i>	<b>October</b>	
<b>1972</b>		8-13	SAS, Dallas, Tex.
<b>January</b>		9-13	ICO, Santa Monica, Calif. <i>R. Scott, Perkin-Elmer Corp., Norwalk, Conn.</i>
31-Feb. 3	APS-AAPT, San Francisco <i>W. W. Havens, Jr., 335 E. 45th St., New York, N.Y. 10017</i>	17-20	Optical Society of America, 57th Ann. Mtg., Jack Tar Hotel, San Francisco <i>J. W. Quinn, OSA, 2100 Pa. Ave., N.W., Wash., D.C. 20037</i>
<b>March</b>		23-26	ISA 27th Ann. Conf. & Exhibit, New York <i>ISA HQ, 400 Stanwix St., Pittsburgh, Pa. 15222</i>
1-3	Scintillation and Semiconductor Symp., Shoreham Hotel, Washington, D.C. <i>IEEE, 345 E. 47th St., New York, N.Y. 10017</i>	<b>1973</b>	
6-10	Pittsburgh Conf. on Analytical Chem. and Appl. Spectroscopy, Cleveland Conv. Ctr. <i>E. E. Hodge, Mellon Inst., 4400 Fifth Ave., Pittsburgh, Pa. 15213</i>	<b>October</b>	
<b>April</b>		1-5	SAS, Niagara Falls, N.Y.
9-15	SMPTE 111th Semiann. Conf., Washington, D.C. <i>D. A. Courtney, 9 E. 41st St., New York, N.Y. 10017</i>	<b>1974</b>	
11-14	Optical Society of America, Statler Hilton, NYC <i>J. W. Quinn, OSA, 2100 Pa. Ave., N.W., Washington, D.C. 20037</i>	<b>October</b>	
		7-11	SAS, Indianapolis, Ind.
		<b>1976</b>	
		<b>October</b>	
		8-12	SAS, Philadelphia, Pa.